12th AIAA/CEAS Aeroacoustics Conference (27th AIAA Aeroacoustics Conference)
8 - 10 May 2006, Cambridge, Massachusetts

AIAA 2006-2443

Computation of the noise radiated by jets with laminar/turbulent nozzle-exit conditions

Sébastien Barré[*], **Christophe Bogey**[†] and **Christophe Bailly**[‡]

Laboratoire de Mécanique des Fluides et d'Acoustique

UMR CNRS 5509, Ecole Centrale de Lyon

69134 Ecully, France

Subsonic isothermal round jets at Mach number $M_j = 0.9$ and at the diameter-based Reynolds number $Re_D = 5 \times 10^5$ are computed using compressible Large Eddy Simulation (LES), in order to investigate the effects of nozzle-exit turbulence levels on jet noise. A pipe nozzle is included in the computational domain, and the development of the boundary layer inside the nozzle is calculated. In this way, two jets displaying respectively low and high turbulence levels at the nozzle exit are considered. In the two cases, the levels of fluctuating axial velocity at the nozzle exit are indeed of 0.016 and 0.090 with respect of the jet velocity, while the momentum thickness of the boundary layers is nearly the same. The shear-layer developments and the radiated sound fields obtained for the two jets are found to differ significantly. The shear layer of the jet with low nozzle-exit turbulence levels develops with higher turbulence intensities and a velocity flow field that is more correlated. Coherent annular vortices are also clearly observed only in this jet. Regarding the radiated noise, the jet with high turbulence levels at the nozzle exit provides sound levels and spectra in very good agreement with experimental data obtained for jets at high Reynolds numbers $Re_D \geq 5 \times 10^5$, which are expected to be initially turbulent. The computed jet with low exit turbulence levels is shown to generate more noise, which results from vortex pairings in the shear layer.

I. Introduction

Computational aeroacoustics has made impressive advances over the last decade, and offers new perspectives on jet noise understanding and reduction, as it was pointed out by Tam[1] in 1998. The first challenge to overcome is however to show that the noise radiated by practical jets can be accurately predicted by numerical simulations, directly by solving the unsteady compressible flow motion equations without resorting to *ad hoc* parameters. With this aim in view, the development of Large Eddy Simulation (LES) techniques as well as the increase of computational power have led to significant progress, which are reported for instance in the recent review of Wang *et al.*[2] Among the first LES of subsonic jet noise, the works of Zhao *et al.*,[3] Bogey *et al.*,[4–6] Bodony & Lele[7] and Rembold & Kleiser[8] can be particularly mentioned. They demonstrated the feasibility of the direct computation of jet noise using LES for cold and hot subsonic jets, both for round and rectangular geometries. Due to limitations in computer memory, these simulations could not however include the nozzle body into the computational domain, and the jet inflow was therefore specified by imposing meanflow profiles while adding low-amplitude disturbances to seed the shear-layer turbulence. This results in uncertainties in the numerical predictions, because the jet development and the radiated noise obtained using this approach were shown to depend appreciably on the characteristics of the inflow forcing disturbances.[9]

In order to avoid this issue and to improve LES of jet noise, it appears necessary to get rid of inflow forcing and to include at least the nozzle body into the computational domain. Such computations have been

[*]PhD Student, sebastien.barre@ec-lyon.fr

[†]CNRS Research Scientist, christophe.bogey@ec-lyon.fr

[‡]Professor at Ecole Centrale de Lyon, Senior Member AIAA, christophe.bailly@ec-lyon.fr

performed by DeBonis & Scott,[10] Biancherin *et al.*,[11] Andersson *et al.*[12] and Wu *et al.*,[13] for cold and hot, subsonic and supersonic round jets. Note that DeBonis & Scott[10] provided only flow field results, whereas the other authors determined directly the radiated noise from their LES. In the works above, no artificial forcing is applied near the nozzle exit, but it is not clear if it is sufficient to obtain accurate predictions of the jet flow and its radiated noise. The role of the nozzle in jet development and noise generation mechanisms is indeed still discussed. The presence of the nozzle is for instance known to be required for the investigation of the screech tones generated in supersonic jets, resulting from a feedback loop closing at the nozzle lip, as shown by the numerical achievements of Shen and Tam,[14] Al-Qadi & Scott,[15] Li & Guo[16] and Berland *et al.*[17] However, for the mixing noise that is generated by the turbulence developing in the jet, the presence of the nozzle alone might not be enough to provide reliable results, because the properties of the boundary layer at the nozzle exit are likely to have significant effects on the jet flow, and therefore have to be carefully considered.

In round jets, the characteristics of the boundary layer at the nozzle exit are actually observed to vary considerably, especially with the diameter-based Reynolds number Re_D. Zaman[18] for exemple noticed experimentally that jets can be expected to be initially laminar for $\mathrm{Re}_D \leq 10^5$, but initially turbulent for $\mathrm{Re}_D \geq 5 \times 10^5$. The resulting changes in the fluctuation levels at the nozzle exit are consequently very important, and affect the mean and turbulent development of the shear layer, in particular, according to Hussain & Zedan,[19] in a much more dramatic way than the variations in the initial momentum thickness do. Husain and Hussain[20] further reported that the peaks of turbulence intensity in the developing shear layer are higher in an initially laminar jet than in an initially turbulent jet, which is expected to have an impact on the noise generated by the jets. Near-field measurements of Zaman[21] and LES fields of Bogey & Bailly[9] indeed support that there are strong links between the peaks of turbulence in the shear layer and the sound sources. As it was suggested by Crighton[22] in the early eighties, the state of the nozzle-exit boundary layer may thus modify jet-noise generation mechanisms. The result for an initially laminar jet can be for instance the presence of additional noise sources, as shown experimentally by Zaman,[23] Bridges & Hussain[24] and Viswanathan.[25] Zaman[23] in particular demonstrated clearly that an initially laminar jet emits more noise than an initially turbulent jet, and attributes this additional noise to vortex pairings in the transitional shear layer. At this point, it is tempting to relate this additional noise to the overestimation of the sound pressure levels that is often obtained in LES of transitional jets at high Reynolds numbers, with or without nozzle, and reported notably by Bogey & Bailly[5] and by Biancherin *et al.*[11]

In the present work, the effects of nozzle-exit turbulence levels on the prediction of the noise radiated by subsonic isothermal round jets at Mach number $\mathrm{M}_j = U_\mathrm{j}/c_\mathrm{j} = 0.9$ and Reynolds number $\mathrm{Re}_D = U_\mathrm{j} D/\nu = 5 \times 10^5$ are investigated (U_j and D are the jet inflow velocity and diameter, c_j is the speed of sound, ν is the molecular kinematic viscosity). With this in mind, two jets and their associated sound fields are computed by compressible LES using low-dissipation and low-dispersion numerical schemes, on a computational grid including a pipe flow. The development of the boundary layer along the pipe is calculated in order to obtain significant turbulence levels at the nozzle exit without using forcing in the jet flow. The two jets considered here exhibit levels of fluctuating axial velocity at the nozzle exit of $0.016U_\mathrm{j}$ and $0.090U_\mathrm{j}$, while the momentum thickness of the boundary layers is nearly the same. To show the influence of the nozzle-exit turbulence levels, the flow fields obtained for the two jets will be compared, with a particular attention given to the shear-layer zone. The near- and far-field sound pressure will be then studied, and compared to experimental data obtained for jets at high Reynolds numbers $\mathrm{Re}_D \geq 5 \times 10^5$, which are expected to be initially turbulent.[18] In this way the agreement between the noise radiated by the jet with the higher turbulence levels at the nozzle exit and that of practical jets will be discussed. The presence of the additional noise observed by Zaman[23] in the jet with low exit turbulence levels will also be tracked.

The paper is organized as follows. In section II, the parameters of the numerical procedure and of the two simulated jets displaying respectively low and high nozzle-exit turbulence levels are defined. The development of the boundary layers along the pipe and the levels of nozzle-exit turbulence are also briefly shown. The flow and sound pressure fields obtained for the two jets are compared in section III: snapshots of vorticity and pressure are presented, properties of the mean flow and turbulent fields are reported, and the sound pressure near and far fields radiated by the jets are characterized in terms of levels, azimuthal cross-correlations and spectra. Concluding remarks are finally drawn in section IV.

II. Simulation parameters

A. Numerical procedure

The turbulent flow and the radiated acoustic field of the jets are both computed directly by compressible LES. The cylindrical filtered Navier-Stokes equations are solved using numerical schemes with low-dispersion and low-dissipation properties.[26,27] The cylindrical geometry allows us to properly describe the jet flow and nozzle. The singularity on the axis is taken into account by the method based on series expansions and proposed by Constantinescu & Lele.[28] The spatial discretization is performed by an eleven-point-stencil finite-difference scheme optimized in the wave-number space ensuring accuracy up to four points per wavelength. An optimized explicit six-stage Runge-Kutta algorithm is used for time integration. To ensure stability, grid-to-grid oscillations are removed by applying explicitly to the flow variables an eleven-point-stencil selective filter. This filtering was designed so that only the short waves discretized by less than four points per wavelength are damped. Therefore it does not affect significantly the resolved scales, and takes account of the dissipative effects of the subgrid scales in a suitable manner. The present LES approach was indeed developed not to artificially decrease the effective Reynolds number of the jet, as it could be the case using more dissipative subgrid modellings.[29,30] Finally, in order to compute the radiated noise directly, non-reflective boundary conditions are implemented, with the addition of a sponge zone in the jet at the outflow.[5]

In the present jet simulations, the computational domain is made of two overlapping grids, as illustrated in figure 1. The nozzle grid has $n_r \times n_\theta \times n_z = 46 \times 48 \times 391$ points, and is used to compute the development of the turbulent boundary layer along the pipe, in order to specify the nozzle-exit conditions. The main grid contains $n_r \times n_\theta \times n_z = 219 \times 48 \times 551$ points, and includes the lips of the nozzle, the jet flow and a part of the acoustic field. In the radial direction, the grids are refined inside the boundary layer and the shear layer, with $\Delta r_0 = 0.009D$. The radial spacing then increases towards the jet centerline at the rate of 2% to reach $\Delta r_{axis} = 0.016D$ on the axis, and outside the jet at the rate of 3% to be $\Delta r_{ac} = 0.066D$ in the acoustic field. The grid thus extends radially up to $r = 8.6D$, and the sound waves are accurately calculated in the acoustic field up to the Strouhal number $\mathrm{St} = fD/U_\mathrm{j} = 3.3$. In the axial direction, the grid spacing is constant in the nozzle and up to $x = 2.6D$ on the main grid, with $\Delta x_0 = 0.016D$. The grid spacing is then stretched at the rate of 2% to reach $\Delta x_{jet} = 0.047D$ up to $x = 16.4D$, where the sponge zone begins. The length of the pipe nozzle is therefore $6.7D$, and that of the overlapping region between the nozzle and the main grids is $0.61D$. The azimuthal direction is discretized by the uniform spacing $\Delta\theta = 2\pi/48$. Finally, to ensure stability, the time step is provided by $\Delta t = 1.1\Delta r_{axis}\Delta\theta/c_0$. The simulation time is $1.02 \times 10^5 \Delta t$, including a transitory period of $2.5 \times 10^4 \Delta t$. The physical time T therefore corresponds to $TU_\mathrm{j}/D = 160$. More details can be found in Barre.[31]

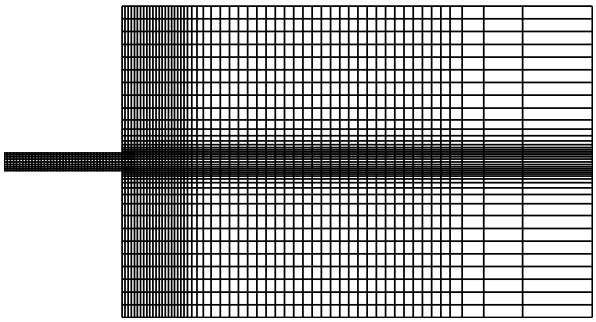

Figure 1. Visualization in the (x, r) plane of the grid used for the jet simulations. Only every tenth line is shown.

B. Jet specifications

Two isothermal jets at Mach number $\mathrm{M_j} = U_\mathrm{j}/c_\mathrm{j} = 0.9$ and Reynolds number $\mathrm{Re}_D = U_\mathrm{j}D/\nu = 5 \times 10^5$ are simulated. In order to study the influence of the initial shear-layer state on the flow development and noise, the peak level of fluctuating axial velocity at the nozzle exit is $0.09U_\mathrm{j}$ in the first jet and $0.016U_\mathrm{j}$ in the second jet, while the initial momentum thickness is about $\delta_\theta = 0.012D$ in the two cases. In what follows,

Table 1. Parameters of the two simulated jets: Mach and Reynolds numbers, and maximum rms levels of the fluctuating axial velocity at $x = 0$ at the nozzle exit.

	M_j	Re_D	$\max(u_{x_{rms}}(x=0))$
jetT	0.9	5×10^5	$0.090U_j$
jetL	0.9	5×10^5	$0.016U_j$

these jets will be respectively referred to as jetT and jetL, as shown in table 1.

For a round jet at Reynolds number $Re_D = 5 \times 10^5$, according to the experiments of Zaman,[18] the boundary layer at the nozzle exit is expected to be turbulent, and its momentum thickness δ_θ is of the order of $10^{-3}D$. Such a very thin boundary layer cannot be discretized with the computers that are currently available to us. In the present LES, a thicker boundary layer is consequently prescribed. More precisely, a laminar boundary layer is imposed at the inflow of the nozzle pipe. It is defined by a polynomial approximation of a Blasius profile characterized by a thickness of $\delta = 0.064D$:

$$U_x(r_w) = U_j \frac{r_w}{\delta}\left[2 - 2\left(\frac{r_w}{\delta}\right)^2 + \left(\frac{r_w}{\delta}\right)^3\right] \quad \text{if } r_w < \delta$$
$$U_x(r_w) = U_j \quad \text{if } r_w \geq \delta$$

where r_w is the distance from the wall. At the inflow, temperature is then determined by a Crocco-Busemann relation. In order to seed the turbulence, random velocity fluctuations with low amplitude are introduced in the boundary layer, at $x = -6.4D$ far upstream inside the nozzle. In wall units, the radial spacing at the wall is $\Delta r^+ = 36$, and the axial spacing is $\Delta x^+ = 63$. Moreover, since $\Delta r_0 = 0.009D$ at the wall, there are only seven points in the boundary layer. Note however that non-centered finite differences and selective filters[27] involving eleven point stencils and accurate up to four points per wavelength are used at the wall boundaries. Despite a relatively coarse grid, turbulent structures are therefore likely to develop in the boundary layer. Keep also in mind that the aim here is not to compute the boundary layer with high fidelity as it can be done in Direct Numerical Simulations (DNS),[32] but to mimic the behaviour of a developing boundary layer so as to obtain a nozzle-exit turbulence resulting from the physics of this flow, and as physical as possible for the LES of jet noise. In this way, results should not be strongly biased by the properties of the initial disturbances as it is the case when forcing is applied in the jet flow.[9] The present method should also allow us to obtain high levels of turbulence at the jet inflow, without generating significant spurious sound pressure waves.

C. Properties of the boundary layers

The properties of the boundary layers developing in the nozzle of jetT and jetL are briefly investigated. The axial evolution of the levels of fluctuating axial velocity $u_{x_{rms}}$ at $r = 0.47D$ along the pipe is shown in figure 2(a). It can be first noticed the difference in amplitude of the random disturbances introduced at $x = -6.4D$ in order to obtain the nozzle-exit turbulence levels reported in table 1. The amplitude of these disturbances is indeed of $0.02U_j$ for jetT, but only of the order of $0.001U_j$ for jetL. These disturbances are naturally growing along the pipe, to provide, at the nozzle exit, the radial profiles of $u_{x_{rms}}$ presented in figure 2(b). As expected, the turbulence levels are important in the boundary layer close to the wall, whereas $u_{x_{rms}} \simeq 0.005U_j$ is found in the centerline region. The peak levels obtained correspond also well to the values given in table 1, that are $0.09U_j$ in jetT and $0.016U_j$ in jetL. Furthermore, in order to check the jet initial conditions, the momentum thickness of the boundary layers at the nozzle exit is also calculated. Thicknesses of $\delta_\theta = 0.013D$ and $\delta_\theta = 0.012D$ are respectively obtained for jetT and jetL.

The radial profiles of the fluctuating axial, radial and azimutal velocities at $x = -0.6D$ close to the nozzle exit are now presented in figure 3 for jetT. The relative shapes of the curves obtained for the different velocity components are in fairly good agreement with the experimental and DNS data reported by Eggels *et al.*[32] for a fully developed turbulent pipe flow at a low Reynolds number. This agreement is however qualitative, because, due to the discretization used in the present LES, the peak levels in jetT are observed farther from the wall than those obtained by Eggels *et al.*[32] The peaks of $u_{x_{rms}}$ noticed by these authors are indeed typically at $r_w^+ \leq 30$, whereas in our LES of jetT, the peak of $u_{x_{rms}}$ is at $r_w^+ = 2\Delta r^+ = 72$.

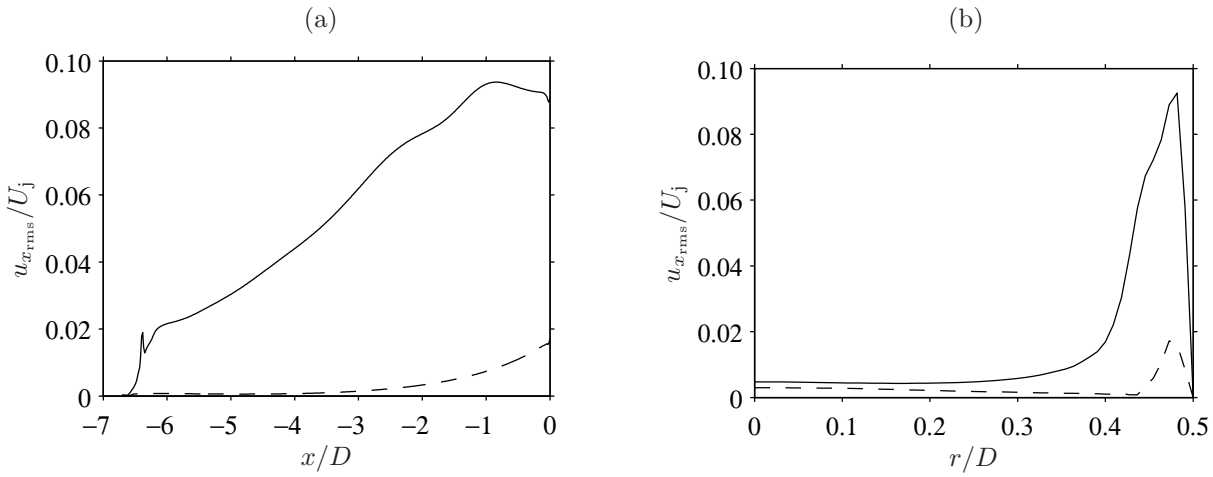

Figure 2. Levels $u_{x_{\rm rms}}$ of the fluctuating axial velocity. (a) Axial evolutions in the nozzle, at $r = 0.47D$ in the boundary layer, and (b) radial profiles at $x = 0$ at the nozzle exit, obtained for: ——— jetT; − − − jetL.

The boundary layers calculated in the present LES are therefore under-resolved. Their developments along the pipe however provide jet initial conditions at the nozzle exit displaying high levels of turbulence, and generated by a part of the physics of the boundary layer, and not entirely from an arbitrary forcing as it was the case in previous simulations.[9]

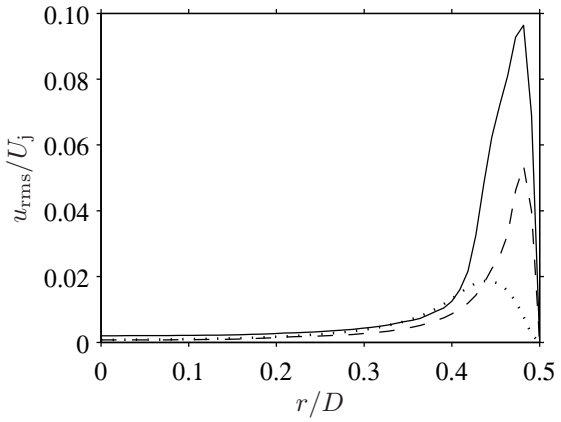

Figure 3. Profiles of the levels of fluctuating axial, radial and azimuthal velocities at $x = -0.6D$ for jetT. ——— axial velocity $u_{x_{\rm rms}}$, ····· radial velocity $u_{r_{\rm rms}}$, − − − azimuthal velocity $u_{\theta_{\rm rms}}$.

III. Results

A. Snapshots of vorticity and pressure

Snapshots of the vorticity fields obtained for jetT and jetL in the shear layer developing after the nozzle are shown in figure 4. For the jet with high initial levels of turbulence, in figure 4(a), small vortical structures are visibly found very close to the nozzle exit, displaying rapidly typical features of three-dimensional turbulence. For the jet with low nozzle-exit turbulence levels, in figure 4(b), the shear layer develops quite differently. It appears indeed laminar up to the location $x \simeq 0.5D$, where coherent vortices are then generated. These vortices are convected in the downstream direction, and pairings occur around $x = 2D$. After the pairings, the shear-layer turbulence then tends to be three-dimensional. Since vortex pairings are known as efficient noise generation mechanisms, the impact on the radiated noise can be expected to be significant. In the present LES, the sound sources likely to be at the origin of an additional noise in initially laminar jets are

observed in jetL but not in jetT.

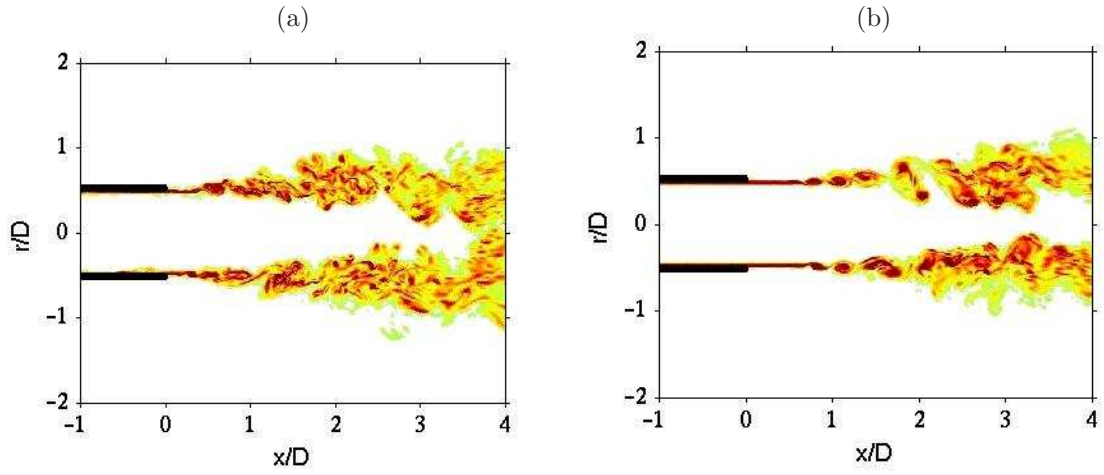

Figure 4. Snapshots in the (x, r) plane of the vorticity norm obtained just downstream of the nozzle exit for: (a) jetT, (b) jetL. The color scale ranges up to the vorticity level of 2×10^5 s^{-1}.

To illustrate the noise radiated by the two simulated jets, snapshots of the vorticity and of the sound pressure fields obtained on the whole computational domain are presented in figure 5. The modelling of the nozzle-exit fluctuations in the present compressible LES does not visibly generate notable spurious acoustic waves. This is of importance especially for jetT in figure 5(a) with initial turbulence intensities of around 10%. Although it can be hazardous to compare two snapshots of pressure, the present acoustic fields clearly show that the sound pressure levels emitted by jetL are higher than those of jetT, in particular in the sideline direction. For jetL in figure 5(b), acoustic waves that appears to originate from the shear-layer zone are seen to dominate the sound field. For jetT in figure 5(a), this kind of waves is however not so predominant. An additional radiation is therefore observed for the jet with low turbulence levels at the nozzle exit with respect to the jet with high turbulence levels. This radiation can reasonably be attributed to the first stage of pairing of the coherent shear-layer vortices. This result agrees very well with the experimental works of Zaman[23] and Bridges & Hussain[24] for initially laminar and turbulent jets.

B. Mean and turbulent flow fields

The mean and turbulent flow fields of the jets are now investigated. The mean axial velocity field and the streamlines around the jet are first represented in Figure 6 for jetT. The streamline pattern is in good agreement with experimental findings, and indicates that the entrainment of the fluid surrounding the jet into the flow occurs in an appropriate manner, and is not obstructed by the boundary conditions.

The length of the potential core x_c, defined here arbitrarily by $u_c(x_c) = 0.95U_\mathrm{j}$ where u_c is the jet mean centerline velocity, is $x_c = 4.7D$ for both jetT and jetL. This value is smaller than corresponding results obtained experimentally for Mach 0.9 jets[33,34] at high Reynolds numbers $\mathrm{Re}_D \geq 5.0 \times 10^5$, which exhibit $x_c \simeq 7D$. This discrepancy is likely due to the difference in momentum thickness at the nozzle exit, since $\delta_\theta = 0.012D$ is specified in the present simulated jets whereas $\delta_\theta \simeq 0.001D$ is expected in experimental jets at such Reynolds numbers.[18]

The variations of the mean axial velocity u_c along the jet centerline are presented in figure 7. The velocity decays obtained for jetT and jetL do not significantly differ, and agree with the velocity decay measured by Lau *et al.*[33] for a jet at $\mathrm{M}_\mathrm{j} = 0.9$ and $\mathrm{Re}_D = 10^6$. Note that this velocity decay was found in a previous work[30] to depend appreciably on the Reynolds number of the flow. The present LES therefore provide results in agreement with the high Reynolds number considered. In addition, the velocity decay appears slightly more rapid in jetL than in jetT. This point may be related to the fact that the rate of decay of the centerline velocity was shown to be somewhat higher in initially transitional jets than in initially turbulent jets.[35,36]

The levels of the fluctuating axial velocity u_{x_rms} on the jet centerline are presented in figure 8. They rapidly increase at the end of the potential core, and reach a peak about at $x = x_c + D$ in jetL, and $x = x_c + 2D$ in jetT. The peak level obtained for jetL is higher than that for jetT ($0.14U_\mathrm{j}$ versus $0.12U_\mathrm{j}$). Both peak values are in the range of experimental data for Mach number 0.9 jets[33,34] at $\mathrm{Re}_D \geq 5.0 \times 10^5$.

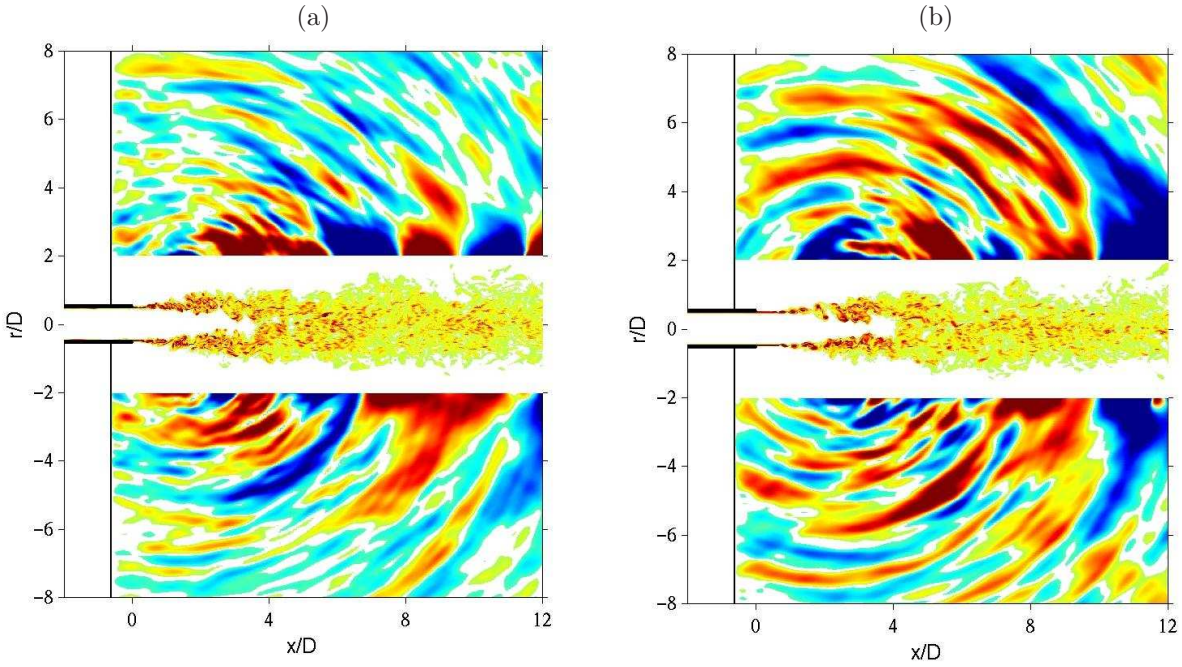

Figure 5. Snapshots in the (x, r) plane of the vorticity norm in the flow and of the fluctuating pressure outside, for: (a) jetT, (b) jetL. The color scales range up to the level of 2×10^5 s^{-1} for the vorticity, and from -100 Pa up to 100 Pa for the pressure.

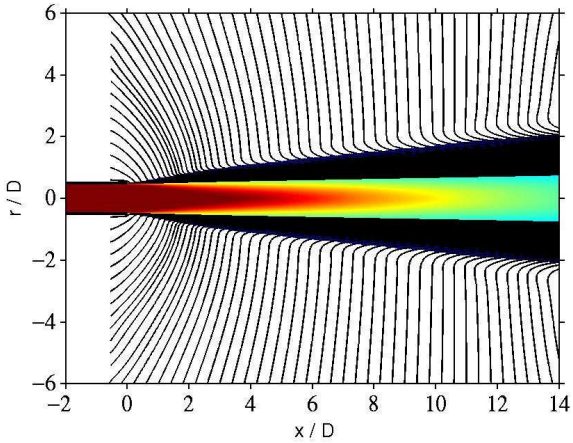

Figure 6. Mean axial velocity field obtained in the (x, r) plane for jetT. The color scale is defined up to the velocity U_j. —— Streamlines.

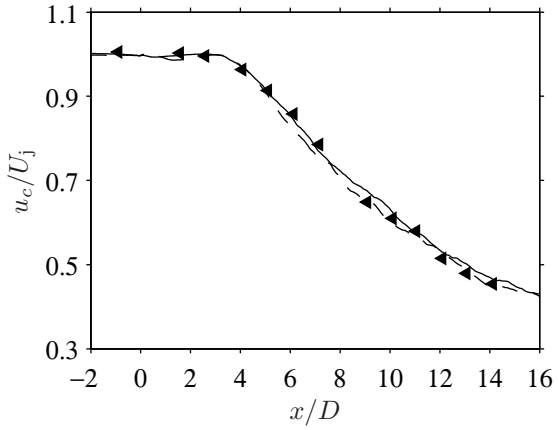

Figure 7. Centerline profiles of mean axial velocity, obtained for: ——— jetT; − − − jetL. Measurements: ◀ Lau *et al.*[33] ($M_j = 0.9$, $Re_D = 10^6$). For the comparison the experimental profiles are shifted in the axial direction with respect to the LES profiles to yield identical core lengths.

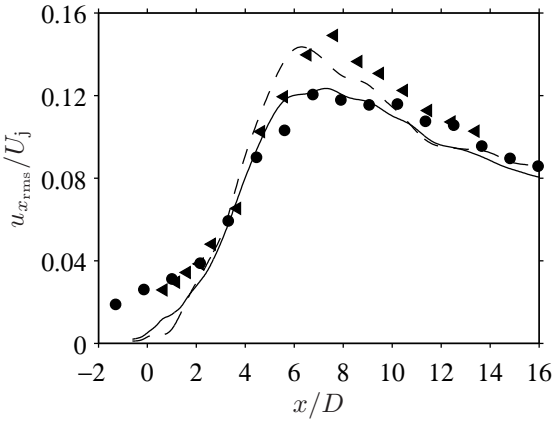

Figure 8. Centerline profiles of the levels u_{x_rms} of the fluctuating axial velocity, obtained for: ——— jetT; − − − jetL. Measurements: ◀ Lau *et al.*[33] ($M_j = 0.9$, $Re_D = 10^6$), ● Arakeri *et al.*[34] ($M_j = 0.9$, $Re_D = 5.0 \times 10^5$). For the comparison the experimental profiles are shifted in the axial direction with respect to the LES profiles.

The very good agreement between the LES profile for jetT and the profile obtained by Arakeri *et al.*[34] using PIV measurements can also be noticed.

We now focus on the turbulence developing in the shear layer. The profiles of the fluctuating axial velocity levels along $r = 0.48D$ are plotted in figure 9. Downstream from the nozzle exit, the values of u_{x_rms} in the shear layer increase very rapidly, reach a peak and then slowly decrease. The level peak is closer to the nozzle, and has a lower amplitude in jetT than in jetL. This behaviour is in agreement with the experimental results of Husain & Hussain,[20] who showed that the turbulence levels in the early shear-layer development are lower in initially turbulent jets than in initially laminar jets. In initially laminar jets, they reported peaks of u_{x_rms} at the axial locations $x \simeq 0.4D$, with levels of about $0.18U_\mathrm{j}$. The development of the shear-layer turbulence in the present LES occurs farther downstream with a stronger intensity. This discrepancy with respect to experiments may result from the relatively thick initial momentum thickness of the shear layer specified in the LES, which can appreciably affect the growth rates of instabilities.[37] It may be also due to the properties of the turbulence at the nozzle exit. In initially turbulent shear layers, Husain and Hussain[20] for instance do not observe peaks of u_{x_rms}, this quantity monotonically increasing along the shear layer. Therefore both jetL and jetT display features of initially transitional jets.

In order to investigate the spacial properties of the shear layer turbulence, azimuthal cross-correlations

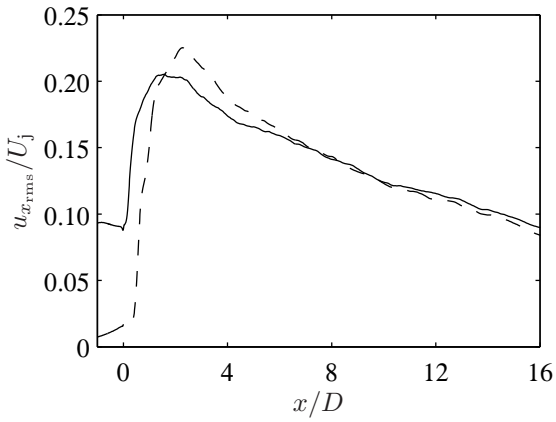

Figure 9. Profiles at $r = 0.48D$ in the shear layer, of the levels $u_{x_{\rm rms}}$ of the fluctuating axial velocity, obtained for: ——— jetT; − − − jetL.

of the fluctuating axial velocity are calculated. The normalized correlation functions are defined by:

$$\mathcal{R}_{xx}^{(\phi)}(x, r, \Delta\phi) = \frac{\langle u'_x(x, r, \phi) u'_x(x, r, \phi + \Delta\phi)\rangle}{\langle u'^2_x(x, r, \phi)\rangle^{1/2} \langle u'^2_x(x, r, \phi + \Delta\phi)\rangle^{1/2}}$$

where ϕ is the azimuthal angle, and $\langle . \rangle$ denotes statistical averaging. They are computed for $r = D/2$ in the shear layer, at the axial locations $x = 0$, $x = D/2$, $x = D$ and $x = 2D$, and they are represented in figure 10(a) for jetT and in figure 10(b) for jetL. For jetT, in the case with high initial turbulence intensities, the correlation levels at $x = 0$ at the nozzle exit are close to 0.5 over the whole range $0 \leq \Delta\phi \leq 180^{\rm o}$, and rapidly decrease at farther downstream locations. The correlations obtained at $x = D/2$, $x = D$ and $x = 2D$ are indeed negligible for $\Delta\phi \geq 20^{\rm o}$. The correlation levels are higher in jetL. At the nozzle exit, $\mathcal{R}_{xx}^{(\phi)} \simeq 1$ is especially found for all azimuthal angles $\Delta\phi$. Downstream, the correlation functions progressively exhibit lower values, to show, at $x = 2D$, levels roughly similar to those in jetT. In jetT, the shear-layer velocity disturbances are therefore weakly correlated azimuthally just after the nozzle exit, *i.e.* from the early stage of the flow development. In jetL, the velocity fluctuations in this transitional region are more correlated. This feature is also indicated by the presence of shear-layer coherent structures in the snapshots of vorticity of figure 4. Moreover the correlations in jetL become similar to those obtained in jetT only at $x = 2D$, after the first vortex pairings.

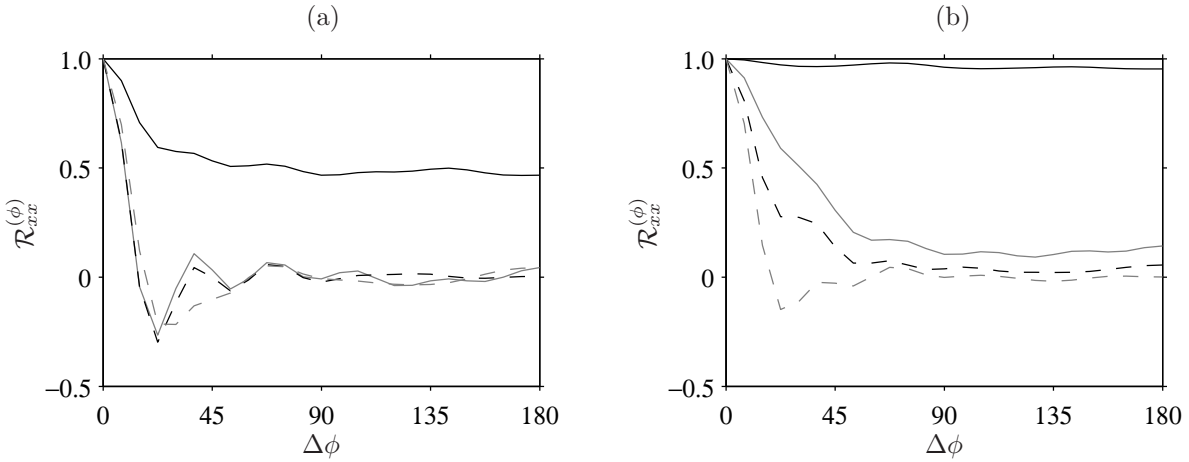

Figure 10. Azimuthal cross-correlation functions of axial velocity, at $r = D/2$ in the shear layer for the axial locations: ——— $x = 0$, ——— $x = D/2$, − − − $x = D$, − − − $x = 2D$, obtained for the jets: (a) jetT, (b) jetL.

C. Sound pressure field

1. *Near acoustic field*

To investigate the noise radiated by the computed jets, properties of the near acoustic fields calculated directly by LES are first presented. The sound pressure levels along the line $r = 7.5D$ are shown in figure 11. They are compared to the experimental data provided by Barré *et al.*[38] for a jet at $M_j = 0.9$ and $Re_D = 7.8 \times 10^5$, that can be expected to be initially turbulent according to Zaman.[18] A good agreement is observed between the sound levels obtained for the jet with significant turbulence levels at the nozzle exit and the measurements. The levels from jetT and from the experiment indeed do not differ by more than 2 dB at all the axial locations considered. With respect to jetT, the jet with low initial turbulence levels is found to generate sound levels higher by 4-5 dB for all emission angles. This behaviour is consistent with the pressure snapshots of figure 5, and corresponds well to the experimental results reported by Zaman[23] and Bridges & Hussain[24] for tripped and untripped subsonic jets. A similar overestimation was also found for the sound levels generated in the sideline direction by high-Reynolds-number, initially laminar jets simulated without nozzle.[5] The present results clearly illustrate the strong impact of the nozzle-exit turbulence levels on the radiated noise. They also characterize quantitatively the additional noise observed in jetL and attributed to vortex pairings occuring in the transitional shear layer.

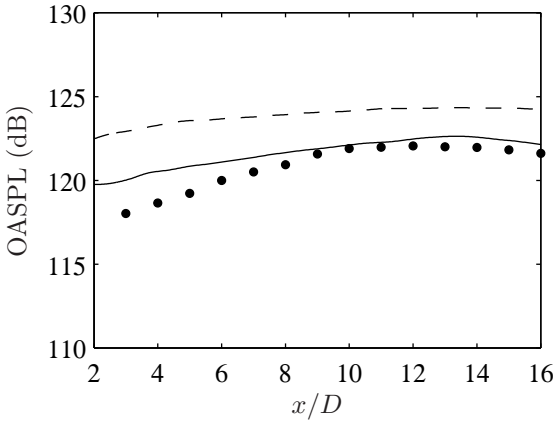

Figure 11. Sound pressure levels obtained along the line $r = 7.5D$, for the jets: ——— jetT, − − − jetL. Measurements: • Barré *et al.*[38] ($M_j = 0.9$, $Re_D = 7.8 \times 10^5$).

To display the spacial structure of the acoustic fields of jetT and jetL, the azimuthal correlation functions of the fluctuating pressure obtained for $r = 7.5D$ from the centerline, at the axial locations $x = 0$ and $x = 15D$, are plotted in figure 12. These functions are calculated in the following way:

$$\mathcal{R}_{pp}^{(\phi)}(x, r, \Delta\phi) = \frac{\langle p'(x, r, \phi) p'(x, r, \phi + \Delta\phi) \rangle}{\langle p'^2(x, r, \phi) \rangle^{1/2} \langle p'^2(x, r, \phi + \Delta\phi) \rangle^{1/2}}$$

In agreement with experimental data[39] and numerical results,[6] the correlation functions are seen to vary remarkably with the angle of radiation with respect to the jet direction. In both jetT and jetL, the correlation levels calculated at $x = 15D$ are indeed high for $0 \leq \Delta\phi \leq 180°$, whereas those at $x = 0$ decrease rapidly with the azimuth (note that the radiation angle, taken from the nozzle exit, is $\theta = 27°$ in the first case, but $\theta = 90°$ in the second case). This classical result supports the presence of two components in jet noise,[1,6] that dominate respectively in the downstream and sideline directions, and can be associated with the turbulence developing randomly in the jet, and with a mechanism intrinsic the jet geometry at the end of the potential core.[40] Moreover the correlation levels are higher in jetL than in jetT. The pressure field obtained in the sideline direction at $x = 0$ decorrelates in particular more slowly in jetL. The azimuthal cross-correlations of the radiated pressure therefore display similarities with the correlations of figure 10 involving the velocity disturbances in the early stage of shear-layer development before the first vortex pairings. This result suggests a direct link between the presence of shear-layer coherent structures and the generation of an excess noise in jetL.

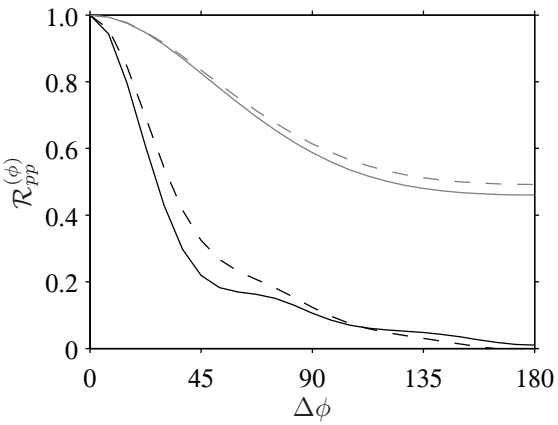

Figure 12. Azimuthal cross-correlation functions of the radiated pressure obtained for the jets: ——— jetT, − − − jetL, at $r = 7.5D$ for the axial locations: $x = 0$ (black curves) and $x = 15D$ (grey curves).

2. Far acoustic field

The investigations of the noise radiated by turbulent flows are usually conducted in the far acoustic field. The near acoustic fields calculated directly by LES for jetT and jetL are therefore now propagated much farther, up to 52 diameters from the jet centerline. Practically, the flow quantities including density, velocity and pressure, provided by LES on two cylindrical surfaces at $r/D = 4$ and $r/D = 6$ surrounding the turbulent jets, are stored. They are then introduced in a propagation solver based on a simplified set of the flow motion equations, as done for instance by Gloerfelt *et al.*[41] for the computation of cavity noise. In the present work, the propagation is carried out by solving the Euler equations using the same numerical schemes and boundary conditions as the LES solver in order to obtain the same accuracy. The propagation grid mesh is uniform and contains $n_r \times n_\theta \times n_x = 529 \times 48 \times 821$ points, and allows us to use a time step 12 times larger than the LES time step. The connection between LES and Euler equations is illustrated in figure 13 with a snapshot of the pressure field obtained using the storage surface at $r/D = 6$. The sound pressure waves appear to be propagated without discontinuity at the joining surface. The results presented in what follows are calculated using the surface at $r/D = 4$, which enables an accurate prediction of the sound waves emitted for angles $\theta \geq 40°$ with respect to the jet direction.

The sound pressure levels calculated along the line located at $r = 20D$ are represented in figure 14. They display the same features as the results obtained at $r = 7.5D$ previously shown in figure 11. The acoustic levels predicted from jetT compare indeed successfully with the experimental data of Barré *et al.*[38] for a jet at $\mathrm{M}_j = 0.9$ and $\mathrm{Re}_D = 7.8 \times 10^5$, whereas the levels from jetL are overestimated by 4-5 dB.

Finally the pressure spectra obtained at a distance of $52D$ from the nozzle exit for angles of $\theta = 40°$ and $\theta = 90°$ with respect to the jet direction are plotted in figures 15(a) and 15(b), respectively. At $\theta = 40°$, the spectrum computed for jetT is in very good agreement with corresponding spectra measured by Barré *et al.*[38] and by Jordan et al.[42] for jets with Reynolds numbers $\mathrm{Re}_D \geq 7.8 \times 10^5$. The maximum difference between numerical and experimental spectra over the range of Strouhal numbers $0.2 \leq \mathrm{St} \leq 3$ is of the order of 1 dB. The peak Strouhal number in jetT is however of $\mathrm{St}_p = 0.33$, that is higher than the $\mathrm{St}_p \simeq 0.20$ observed in experiments. As for the spectrum from jetL, it displays the same shape at the spectrum from jetT, but exhibits levels higher by about 1 dB.

At $\theta = 90°$, the discrepancies between the spectra from jetT and jetL are more significant. With respect to jetT, the spectrum from jetL increases in amplitude, and is characterized by higher-frequency components with a peak Strouhal number at $\mathrm{St}_p = 0.7$. Zaman[23] and Bridges & Hussain[24] in their experiments conducted on tripped/untripped jets observed similar high-frequency peaks in the sideline pressure spectra for untripped jets. In terms of Strouhal number based on the initial momentum thickness of the shear layer $\mathrm{St}_\theta = f\delta_\theta/U_j$, these peaks were in the range of 0.005-0.007. In jetL, the frequency peak is found to correspond to a value of $\mathrm{St}_\theta = f\delta_\theta/U_j = 0.0084$, which is half the value of 0.017 predicted by the linear theory[37] as the most unstable frequency in a laminar shear layer. This shows a link between the first stage of pairing of the shear-layer vortices and the additional noise in jetL. Moreover, with respect to the experimental data,[38,42,43] the spectrum from jetT compares well for low Strouhal numbers $\mathrm{St} \leq 0.4$, but displays overestimated levels for

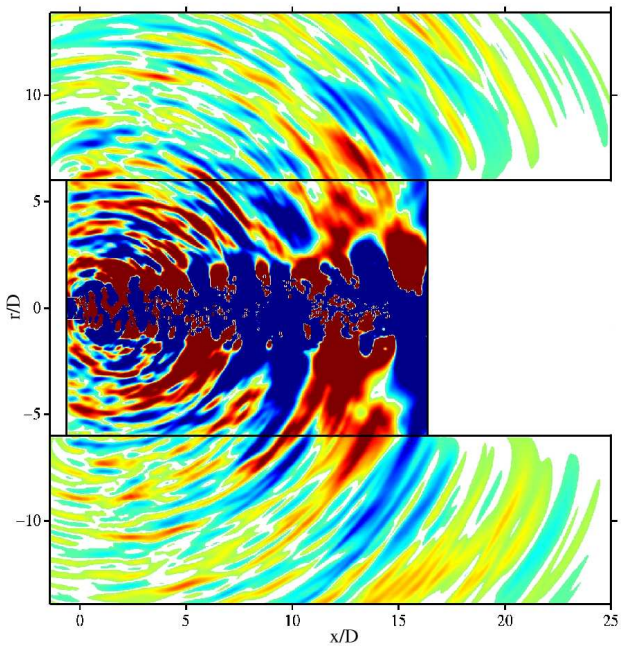

Figure 13. Snapshot in the (x, r) plane of the fluctuating pressure field obtained for jetT. In the central region: pressure field provided by the LES computation, on the periphery: pressure field given by the propagation solver based the Euler equations.

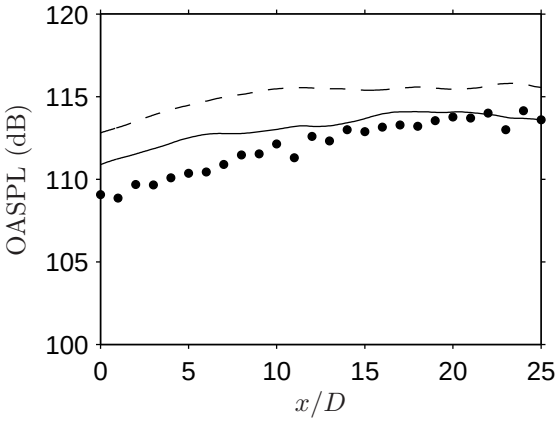

Figure 14. Sound pressure levels obtained along the line $r = 20D$, for the jets: ——— jetT, − − − jetL. Measurements: ● Barré *et al.*[38] ($M_j = 0.9$, $Re_D = 7.8 \times 10^5$).

higher frequencies, The Strouhal peak is thus $St_p = 0.4$ in jetT, instead of $St_p = 0.3$ in experiments. The origin of this discrepancy is to be investigated, but it may be reasonably associated with the properties of the nozzle-exit boundary layer. In jetT, the initial momentum thickness is in particular notably larger than in experiments, and the flow is not fully turbulent at the nozzle exit, as illustrated by the profiles of turbulence intensities along the shear layer in figure 9.

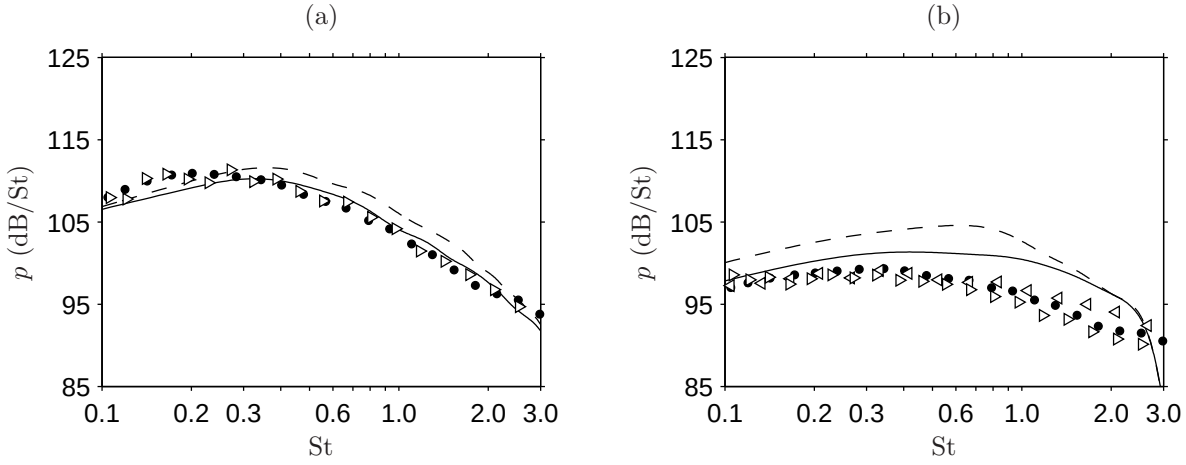

Figure 15. Sound pressure spectra obtained at $52D$ from the nozzle exit for radiation angles: (a) $\theta = 40°$, (b) $\theta = 90°$, for the jets: ——— jetT, − − − jetL. Measurements: • Barré *et al.*[38] ($Re_D = 7.8 \times 10^5$), ▷ Jordan et al.[42] ($Re_D = 10^6$), ◁ Tanna[43] ($Re_D = 10^6$).

IV. Conclusion

The present LES of round jets at Mach number $M_j = 0.9$ and Reynolds number $Re_D = 5 \times 10^5$ show the influence of the levels of turbulence at the nozzle exit on the flow development and noise. This influence is especially found to be significant on the shear layer development and on the sideline sound field. For low turbulence levels at the nozzle exit, coherent structures develop in the shear layer, and their pairings radiate an additional noise likely to increase the sound levels by 4-5 dB. However, for high exit turbulence levels, no pairing seems to occur, and the sound field compares successfully with results obtained experimentally for jets at high Reynolds numbers, that are expected to be initially fully turbulent. For the computation of practical jets, the presence of the nozzle alone therefore appears not sufficient, and turbulent initial conditions are necessary to obtain relevant results.

The difficulty is to generate physical turbulent conditions at the jet nozzle exit at an affordable computational cost, without producing spurious sound waves. One method is to calculate the development of the boundary layer inside the nozzle, as it is proposed and carried out in the present paper, which however implies very fine discretization at the wall boundaries. Moreover, in order to improve the accuracy of predictions, there is a need to better take into account the initial characteristics of practical jets. In particular, boundary layers with smaller momentum thickness and fully turbulent conditions at the nozzle exit will have to be considered in future simulations.

Acknowledgments

The first author is grateful to the Centre National d'Etudes Spatiales (CNES) for financial support. The authors also gratefully acknowledge the Institut du Développement et des Ressources en Informatique Scientifique (IDRIS - CNRS) for providing computing time and for its technical assistance.

References

[1]Tam, C.K.W., "Jet noise: since 1952," *Theoret. Comput. Fluid Dynamics*, Vol. 10, 1998, pp. 393-405.

[2]Wang, M., Freund J.B, and Lele, S.K. "Computational prediction of flow-generated sound," *Annu. Rev. Fluid. Mech.*,

Vol. 38, 2006, pp. 483-512.

[3]Zhao, W., Frankel, S.H., and Mongeau, L., "Large eddy simulations of sound radiation from subsonic turbulent jets," *AIAA Journal*, Vol. 39, No. 8, 2001, pp. 1469-1477.

[4]Bogey, C., Bailly, C., and Juvé, D., "Noise investigation of a high subsonic, moderate Reynolds number jet using a compressible LES," *Theoret. Comput. Fluid Dynamics*, Vol. 16, No. 4, 2003, pp. 273-297.

[5]Bogey, C. and Bailly, C., "Computation of a high Reynolds number jet and its radiated noise using LES based on explicit filtering," *Computers and Fluids*, 2006 (available online).

[6]Bogey, C. and Bailly, C., "Investigation of downstream and sideline subsonic jet noise using Large Eddy Simulations," *Theoret. Comput. Fluid Dynamics*, Vol. 20, No. 1, 2006, pp. 23-40.

[7]Bodony, D.J. and Lele, S.K., "On using large-eddy simulation for the prediction of noise from cold and heated turbulent jets," *Phys. Fluids*, Vol. 17, 085103, 2005, pp. 1-18.

[8]Rembold, B. and Kleiser, L., "Noise prediction of a rectangular jet using Large-Eddy Simulation," *AIAA Journal*, Vol. 42, No. 9, 2004, pp. 1823-1831.

[9]Bogey, C. and Bailly, C., "Effects of inflow conditions and forcing on a Mach 0.9 jet and its radiated noise," *AIAA Journal*, Vol. 43, No. 5, 2005, pp. 1000-1007.

[10]DeBonis, J.R. and Scott, J.N., "Large-Eddy Simulation of a turbulent compressible round jet," *AIAA Journal*, Vol. 40, No. 7, 2002, pp. 1346-1354.

[11]Biancherin, A., Lupoglazoff, N., Vuillot, F., and Rahier, G., "Comprehensive 3D unsteady simulations of subsonic and supersonic hot jet flow-fields. Part 2: acoustic analysis," AIAA Paper 2002-2600.

[12]Andersson, N., Eriksson, L.-E, and Davidson, L., "Large-Eddy Simulation of subsonic turbulent jets and their radiated sound," *AIAA Journal*, Vol. 43, No. 9, 2005, pp. 1899-1912.

[13]Wu, X., Tristanto, I.H., Page G.J. and McGuirk J.J., "Influence of nozzle modelling in LES of turbulent free jets," AIAA Paper 2005-2883.

[14]Shen, H. and Tam, C.K.W, "Three-Dimensional Numerical Simulation of the Jet Screech Phenomenon," *AIAA Journal*, Vol. 40, No. 1, 2002, pp. 33-41.

[15]Al-Qadi, I.M.A. and Scott, J.N., "High-order three dimensional numerical simulation of a supersonic rectangular jet," AIAA Paper 2003-3238.

[16]Li, X.D. and Gao, J.H., "Numerical simulation of three-dimensional supersonic jet screech tones," AIAA Paper 2005-2882.

[17]Berland, J., Bogey, C., and Bailly, C., "Large Eddy Simulation of screech tone generation in a planar underexpanded jet," AIAA Paper 2006-2496.

[18]Zaman, K.B.M.Q., "Far-field noise of a subsonic jet under controlled excitation," *J. Fluid Mech.*, Vol. 152, 1985, pp. 83-111.

[19]Hussain, A.K.M.F. and Zedan, M.F., "Effects of the initial condition on the axisymmetric free shear layer: Effects of the initial fluctuation level," *Phys. Fluids*, Vol. 21, No. 9, 1978, pp. 1475-1481.

[20]Husain, Z.D. and Hussain, A.K.M.F., "Axisymmetric mixing layer: influence of the initial and boundary conditions," *AIAA Journal*, Vol. 17, No. 1, 1979, pp. 48-55.

[21]Zaman, K.B.M.Q., "Flow field and near and far sound field of a subsonic jet," *J. Sound Vib.*, Vol. 106, No. 1, 1986, pp. 1-16.

[22]Crighton, D.G., "Acoustics as a branch of fluid mechanics," *J. Fluid Mech.*, Vol. 106, 1981, pp. 261-298.

[23]Zaman, K.B.M.Q., "Effect of the initial condition on subsonic jet noise," *AIAA Journal*, Vol. 23, No. 9, 1985, pp. 1370-1373.

[24]Bridges, J.E. and Hussain, A.K.M.F., "Roles of initial conditions and vortex pairing in jet noise," *J. Sound Vib.*, Vol. 117, No. 2, 1987, pp. 289-311.

[25]Viswanathan, K., "Aeroacoustics of hot jets," *J. Fluid Mech.*, Vol. 516, 2004, pp. 39-82.

[26]Bogey, C., and Bailly, C., "A family of low dispersive and low dissipative explicit schemes for flow and noise computations," *J. Comput. Phys.*, Vol. 194, No. 1, 2004, pp. 194-214.

[27]Berland, J., Bogey, C., and Bailly, C., "Optimized explicit schemes: matching and boundary schemes, and 4th-order Runge-Kutta algorithm," AIAA Paper 2004-2814.

[28]Constantinescu, G.S. and Lele, S.K., "A highly accurate technique for the treatment of flow equations at the polar axis in cylindrical coordinates using series expansions," *J. Comput. Phys.*, Vol. 183, 2002, pp. 165-186.

[29]Bogey, C. and Bailly, C., "Decrease of the effective Reynolds number with eddy-viscosity subgrid-scale modeling," *AIAA Journal*, Vol. 43, No. 2, 2005, pp. 437-439.

[30]Bogey, C. and Bailly, C., "Large Eddy Simulations of round free jets using explicit filtering with/without dynamic Smagorinsky model," To appear in *Int. J. Heat and Fluid Flow*, 2006. See also in proceedings of Turbulence and Shear Flow Phenomena-4, Vol. 2, 2005, pp. 817-822.

[31]Barré, S., "Etude numérique et expérimentale du bruit aérodynamique avec application aux jets ronds subsoniques," Ph.D. Thesis, Ecole Centrale de Lyon, ECL-No.2006-09, 2006.

[32]Eggels, J.G.M., Unger, F., Weiss, M.H., Westerweel, J., Adrian, R.J., Friedrich, R., and Nieustadt, F.T.M., "Fully developed turbulent pipe flow: a comparison between direct numerical simulation and experiment," *J. Fluid Mech.*, Vol. 268, 1994, pp. 175-209.

[33]Lau, J.C., Morris, P.J., and Fisher, M.J., "Measurements in subsonic and supersonic free jets using a laser velocimeter," *J. Fluid Mech.*, Vol. 93, No. 1, 1979, pp. 1-27.

[34]Arakeri, V.H., Krothapalli, A., Siddavaram, V., Alkislar, M.B., and Lourenco, L., "On the use of microjets to suppress turbulence in a Mach 0.9 axisymmetric jet," *J. Fluid Mech.*, Vol. 490, 2003, pp. 75-98.

[35]Raman, G., Rice, E.J., and Reshotko, E., "Mode spectra of natural disturbances in a circular jet and the effect of acoustic forcing," *Exp. Fluids*, Vol. 17, 1994, pp. 415-426.

[36]Xu, G. and Antonia, R.A., "Effects of different initial conditions on a turbulent free jet," *Exp. Fluids*, Vol. 33, 2002, pp. 677-683.

[37]Michalke, A., "Survey on jet instability theory," *Prog. Aerospace Sci.*, Vol. 21, 1984, pp. 159-199.

[38]Barré, S., Fleury, V., Bogey, C., Bailly, C., and Juvé, D., "Experimental study of the properties of near-field and far-field jet noise," AIAA Paper 2006-2443.

[39]Maestrello, L., "Two points correlations of sound pressure in the far field of a jet: Experiment," NASA-TMX-72835, 1976.

[40]Bogey, C. and Bailly, C., "Investigation of sound sources in subsonic jets using causality methods on LES data," AIAA Paper 2005-2995.

[41]Gloerfelt, X., Bogey, C., and Bailly, C., 2003, "Numerical evidence of mode switching in the flow-induced oscillations by a cavity," *International Journal of Aeroacoustics*, Vol. 2, No. 2, pp. 193-217.

[42]Jordan, P., Gervais, Y., Valière, J.-C., and Foulon, H., "Final results from single point measurements," Project deliverable D3.4, JEAN - EU 5th Framework Programme, G4RD-CT2000-00313, 2002.

[43]Tanna, H.K., "An experimental study of jet noise. Part I: Turbulent mixing noise," *J. Sound Vib.*, Vol. 50, No. 3, pp. 405-428.